Towards improved drug action : target binding kinetics and functional efficacy at the mGlu2 receptor

Doornbos, M.L.J.

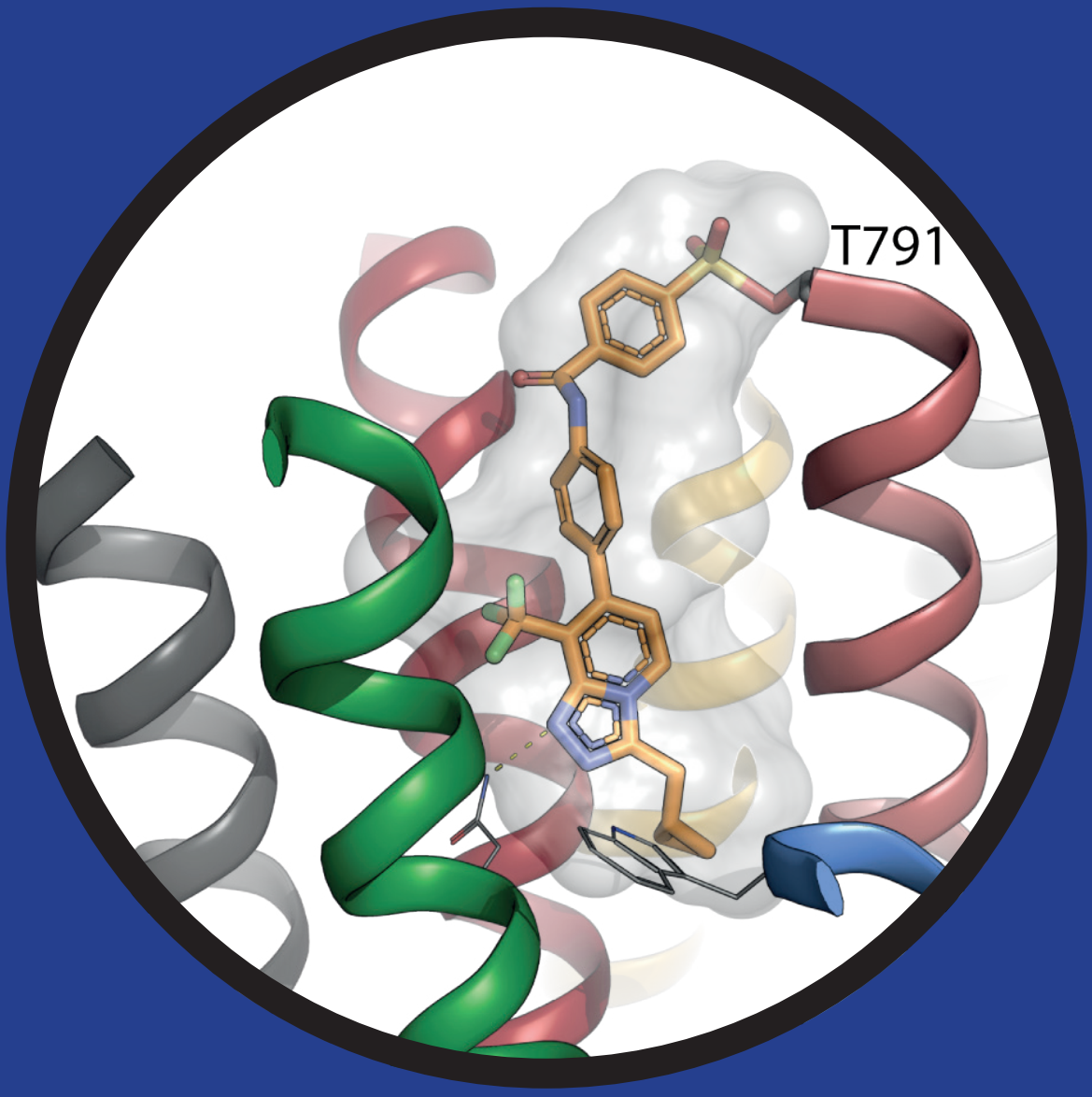
T791

CHAPTER 5

A covalent allosteric probe for the metabotropic glutamate receptor 2: Design, synthesis and pharmacological characterization

Maarten L J Doornbos, Xuesong Wang, Sophie C Vermond, Luc Peeters, Laura Pérez-Benito, Andrés A Trabanco, Hilde Lavreysen, José María Cid, Laura H Heitman, Gary Tresadern & Adriaan P IJzerman

Journal of Medicinal Chemistry.
Publication Date (Web) March 1, 2018.
doi:10.1021/acs.jmedchem.8b00051.

5

ABSTRACT

Covalent labelling of G protein-coupled receptors (GPCRs) by small molecules is a powerful approach to understand binding modes, mechanism of action, pharmacology and even facilitate structure elucidation. We report the first covalent positive allosteric modulator (PAM) for a class C GPCR, the $mGlu_2$ receptor. Three putatively covalent $mGlu_2$ PAMs were designed and synthesized. Pharmacological characterization identified **2** to bind the receptor covalently. Computational modelling combined with receptor mutagenesis revealed $T791^{7.29x30}$ as the likely position of covalent interaction. We show how this covalent ligand can be used to characterize the PAM binding mode and that it is a valuable tool compound in studying receptor function and binding kinetics. Our findings advance the understanding of the $mGlu_2$ PAM interaction and suggest **2** is a valuable probe for further structural and chemical biology approaches.

INTRODUCTION

Over the last years covalent ligands for G protein-coupled receptors (GPCRs) have re-emerged as valuable tool compounds to characterize the structure, expression pattern and function of these proteins.[1] A major obstacle in GPCR structure elucidation using crystallization is the dynamic behavior of their seven-transmembrane (7TM) domain, especially when in the active state.[2] Covalent ligands can stabilize the 7TM domain of the receptor without the likelihood of dissociation from the binding site. The use of covalent ligands for structure elucidation has been taken as an approach to facilitate receptor crystallization, as was shown recently for the crystal structures of the adenosine A_1 and multiple beta 2 adrenergic receptors amongst others.[3,4] Beyond structural considerations, covalent molecules are valuable pharmacological tools useful for further understanding of binding modes, and other chemical biology and proteomics applications.

The metabotropic glutamate (mGlu) receptors belong to the class C GPCRs and are activated by glutamate, the most abundant neurotransmitter.[5] The mGlu receptors are obligatory dimers and are characterized by their large extracellular Venus flytrap (VFT) domain - binding endogenous glutamate - which is connected to the 7TM domain via a cysteine rich domain.[6] For mGlu receptors, allosteric modulators that bind in the 7TM domain are pursued widely for drug discovery as they are typically more subtype-selective than orthosteric ligands and only function in the presence of endogenous agonist.[7] Positive allosteric modulation of the $mGlu_2$ receptor has been shown to be a potential strategy for the treatment of neurological disorders such as schizophrenia and anxiety.[8] Although the structure of the extracellular domain of the $mGlu_2$ receptor is known,[9] the current understanding of the structure of the 7TM domain is based on the crystal structures of the $mGlu_1$ and $mGlu_5$ 7TM domains, which were crystallized in an inactive state with a negative allosteric modulator (NAM) bound in the allosteric binding pocket.[10–12]

We have had a long-standing interest in $mGlu_2$ receptor PAMs leading to characterization of multiple medicinal chemistry series[13,14] that were also studied with site-directed mutagenesis.[15,16] We have further characterized the binding kinetics and pharmacology of selected leads in **chapters 2 and 4**.[17,18] Robust *in vivo* pharmacodynamic effects were observed in several animal models with some molecules such as 1-Butyl-3-chloro-4-(4-phenyl-1-piperidinyl)-(1*H*)-pyridone (JNJ-40411813/ADX71149) advancing to human clinical trials.[19–22] Despite this, further and more rigorous approaches to understand $mGlu_2$ PAM binding and receptor pharmacology are needed. In this study we have designed and synthesized three novel putatively covalent $mGlu_2$ PAMs based on computational approaches and previous understanding of the PAM binding mode. These compounds were fully characterized *in vitro*, resulting in the

identification of 4-[[4-[3-(Cyclopropylmethyl)-8-(trifluoromethyl)-[1,2,4]triazolo[4,3-a]pyridin-7-yl]phenyl]carbamoyl]benzenesulfonyl fluoride (**2**) as a covalently binding $mGlu_2$ PAM. The binding mode was studied using computational docking, which identified several amino acid residues that potentially formed the covalent interaction. Using site-directed mutagenesis $T791^{7.29x30}$ was confirmed as the residue responsible for the covalent interaction.

RESULTS AND DISCUSSION

CHEMISTRY

Based on a series of analogues of 3-(cyclopropylmethyl)-7-[(4-phenyl-1-piperidinyl) methyl]-8-(trifluoromethyl)-1,2,4-triazolo[4,3-a]pyridine (**1**, JNJ-46281222)[23] we recently developed a novel series of $mGlu_2$ PAMs bearing the 7-aryl-1,2,4-triazolo[4,3-a]pyridine as the core structure, also including the molecules described in **chapter 4**.[13,17] This scaffold was used to design three novel putative covalent $mGlu_2$ PAMs for which the fluorosulfonyl moiety was chosen as a reactive warhead. A 4-fluorosulfonyl-phenyl ring was connected to the 7-phenyl-1,2,4-triazolo[4,3-a]pyridine-core via an amide linker to the phenyl ring at the 4-position (**2**), the 3-position (**3**) or the 4-position with a methylene spacer in between to increase flexibility (**4**), as depicted in figure 1. The synthesis of target compounds **2–4** is shown in Scheme 1. They were prepared via Suzuki coupling of the 7-chlorotriazolopyridine **5**[24] with the corresponding commercially available boronic acids (**6a-c**) and subsequent amide formation of **7a-c** with the commercially available chemoreactive group. This electrophilic fluorosulfonyl moiety was chosen as a warhead to achieve a covalent interaction with a nucleophilic amino acid at the allosteric binding pocket of the $mGlu_2$ receptor. This moiety has been widely used and was chosen for its wide reactivity to various nucleophilic residues: serine, threonine, tyrosine, lysine, cysteine and histidine.[25]

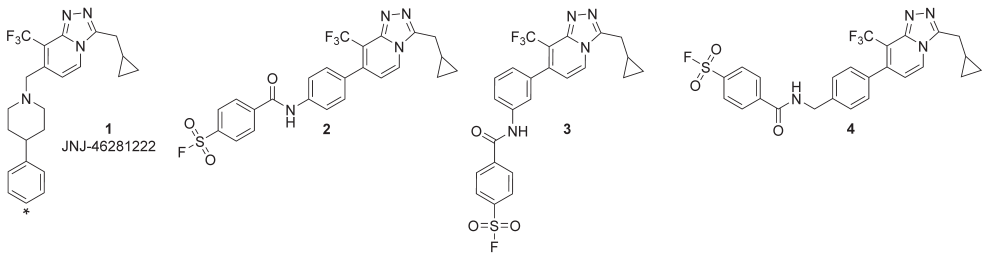

Figure 1. Structure of **1** and novel $mGlu_2$ PAMs **2-4**. The position of the tritium label of [^{3}H]-**1** is denoted by *.

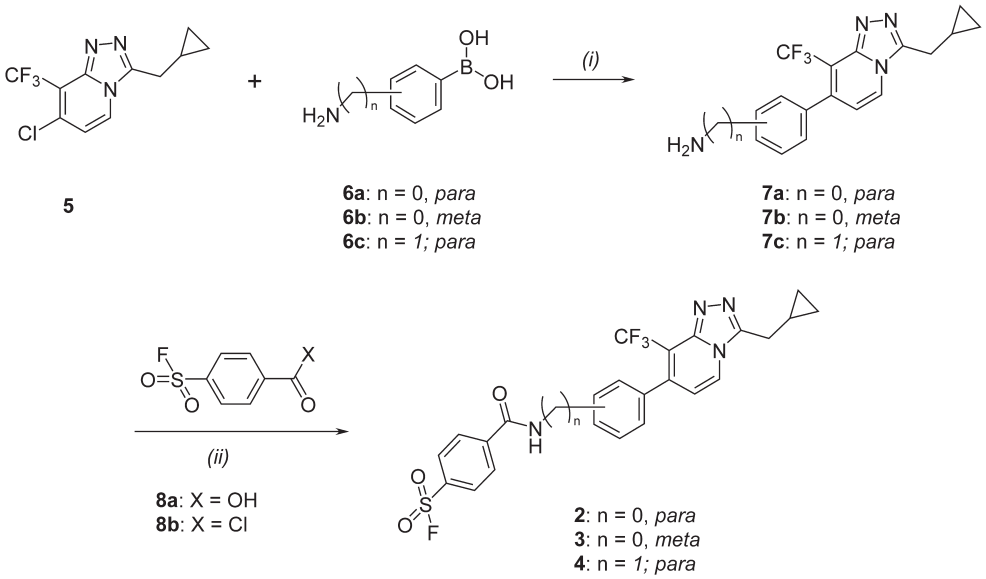

Scheme 1. Synthesis of compounds **2–4.** *Reagents and conditions:* (i) $Pd(PPh_3)_4$, $NaHCO_3$, H_2O/1,4-dioxane, 150 °C, 10-15 min, microwave, 61-68% for **7a-c**. (ii) a) **8a**, HATU, DIPEA, DMF, rt, 3h, 68-75% for **2** and **3** b) **8b**, 1,4-dioxane, 90°C, 30 min, 33% for **4**.

BIOLOGY AND STRUCTURE-REACTIVITY CONSIDERATIONS

Firstly, the potency of the compounds to enhance the effect of glutamate at its EC_{20} was determined using a [^{35}S]GTPγS assay. Reference PAM **1**, showed a high potency (Table 1; pEC_{50} 7.74 ± 0.03). Compounds **2**-**4** were all able to increase the response of the EC_{20} glutamate concentration to a similar level as **1** and thus behaved as functional $mGlu_2$ PAMs with potencies of around 100 nM for **2** and **3** (pEC_{50} values of 6.80 ± 0.06 and 6.80 ± 0.04, respectively). The highest potency was found for **4**, with a pEC_{50} value of 7.82 ± 0.06.

Subsequently, the apparent affinities of the compounds were determined in a [^{3}H]JNJ-46281222 displacement assay (Table 1). The pK_i value of 8.12 ± 0.19 for **1** was close to its pEC_{50} value. Also, **2** and **3** had pK_i values close to their pEC_{50} values, 7.21 ± 0.11 and 6.95 ± 0.11, respectively. Compound **4** had the highest affinity with a pK_i value of 8.24 ± 0.08.

The pEC_{50} and pK_i values (7.74 ± 0.03 and 8.12 ± 0.13, respectively) of **1** were similar to those reported in **chapter 2**.[18] The potency and affinity parameters of **2**-**4** compared favorably with the well-studied **1**, which was one of the most potent compounds identified from the same triazolopyridine scaffold and was used as a control throughout the study. Even though the fluorosulfonyl moiety at the distal tail in **2**-**4** was more bulky and hydrophilic than the unsubstituted phenyl of **1** and the other compounds studied previously and in **chapter 4**,[17,23] the affinity and potency values were only reduced approximately 10-fold for **2** and **3** compared to **1** and not at all for **4**. The shift of the 4-fluorosulfonyl-phenyl ring from the 4-position in **2** to the 3-position in **3** did not change the potency and affinity, whereas the greater flexibility of the methylene spacer in **4** most likely resulted in its increased potency and affinity compared

to **2**. Selectivity of this series of $mGlu_2$ PAMs was good. Representative **3** showed no activity at $mGlu_{1,3,5,8}$ (Table S1).

Table 1. Functional activity (pEC_{50}), affinity (pK_i) and kinetic parameters (k_{on}, k_{off}, RT) for $mGlu_2$ PAMs **1-4**

	pEC_{50}[a]	pK_i[a]	pK_i (3 hr pre-incubation)[a]	k_{on} (M^{-1} s^{-1})[a]	k_{off} (s^{-1})[a]	RT (min)[a, b]
1	7.74 ± 0.03	8.12 ± 0.13	8.12 ± 0.19	(1.2 ± 0.072) x 10^{6}, [c]	0.0013 ± 0.0002[c]	12 ± 2.3[c]
2	6.80 ± 0.06	7.21 ± 0.11	8.21 ± 0.14*	'(3.2 ± 1.2) x 10^{3}'	'(3.2 ± 3.1) x 10^{-13}'	'((5.2 ± 4.9) x 10^{10})'
3	6.80 ± 0.04	6.95 ± 0.11	6.78 ± 0.09	(2.1 ± 0.77) x 10^{4}	0.00091 ± 0.00033	18 ± 6.7
4	7.82 ± 0.06	8.24 ± 0.08	8.38 ± 0.10	(2.2 ± 0.17) x 10^{5}	0.00057 ± 0.00016	29 ± 8.3

[a] Values represent the mean ± SEM of at least three individual experiments, performed in duplicate. [b] RT (min) = $1/(60*k_{off})$. [c] As described in **chapter 4**.[17] * <0.01, unpaired student's t-test compared to co-incubation.

Since a covalent interaction would induce insurmountable binding to the allosteric binding site, we set up a radioligand displacement assay using a 3 hour pre-incubation of CHO-K1_ $hmGlu_2$ membranes with increasing concentrations of the four PAMs. This pre-incubation was followed by addition of [^{3}H]JNJ-46281222 and a subsequent incubation for 1 hour. Data were compared to the control experiments with no pre-incubation, i.e. co-incubation of the radioligand and the compounds studied.

Compound **1** showed no difference in affinity between the co-incubation and the pre-incubation assays (Table 1; pK_i 8.12 in both cases), indicating that **1** does not bind insurmountably to the allosteric binding pocket. On the contrary, the addition of a pre-incubation step resulted in a 10-fold increase in affinity for **2** (Table 1; Fig. 2A), indicating that this compound binds the receptor insurmountably as no re-equilibration of **2** occurred after addition of [^{3}H] JNJ-46281222. Both **3** and **4** did not reveal a significant shift in receptor affinity when tested in the two-step binding assay, indicating they do not bind the receptor insurmountably. The observation of a shift in affinity of **2** after pre-incubation is in agreement with previously described covalent ligands for the histamine H_4 and adenosine A_{2A} receptors.[26,27]

Competition binding experiments are generally not the preferred method for evaluation of covalent interactions with GPCRs.[28,29] Therefore, the kinetic parameters k_{on} and k_{off} of **1**-**4** were determined (Table 1). The kinetic parameters for **1** were determined in classical [^{3}H] JNJ-46281222 association and dissociation experiments, yielding the association rate constant k_{on} (k_1 = 1.2 x 10^6 $M^{-1}s^{-1}$) and dissociation rate constant k_{off} (k_2 = 0.0013 s^{-1}), leading to a residence time (RT) of 12 minutes. Using these values we determined the kinetic k_{on} (k_3) and k_{off} (k_4) values for **2-4** using a competition association assay based on the Motulsky and Mahan model.[30] In contrast to **1**, **2** showed a much slower on-rate (3.2 x10^3 $M^{-1}s^{-1}$) and a negligible off-rate (3.2 x 10^{-13} s^{-1}), leading to an infinite RT, indicative for irreversible binding.

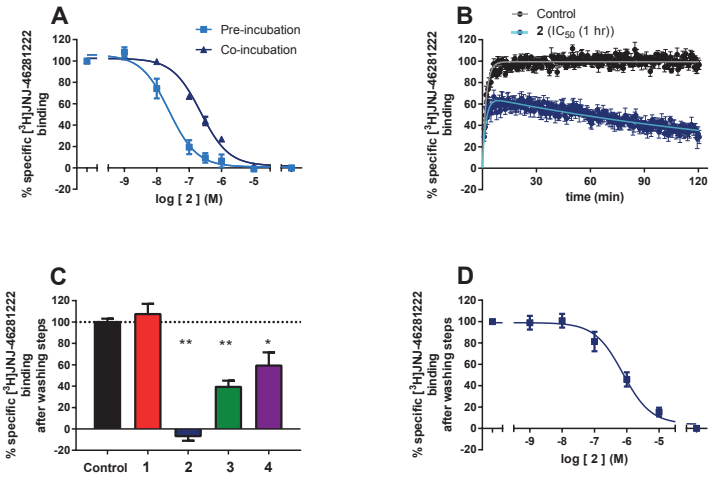

Figure 2. A.) Displacement of [^{3}H]JNJ-46281222 by **2** with and without a pre-incubation of 3 hours. B.) Competition association assay of **2** at its IC_{50} concentration determined in the co-incubation assay. C.) [^{3}H]JNJ-46281222 binding after pre-incubation with a 10x IC_{50} concentration of $mGlu_2$ PAM followed by 4 extensive washing cycles. D.) [^{3}H]JNJ-46281222 binding after pre-incubation with increasing concentrations of **2** followed by 4 extensive washing cycles. Data represent the mean ± SEM of at least three individual experiments performed in duplicate. * p<0.01; ** p<0.0001, one-way ANOVA with Dunnett's post-test compared to control.

The competition association curve of **2** shows an overshoot followed by a declining curve that did not reach equilibrium (Fig. 2B). Compound **3** showed an on-rate of 2.1 x 10^4 $M^{-1}s^{-1}$ and an off-rate of 0.00091 s^{-1}, leading to a RT of 18 minutes, which is comparable to **1**. The on-rate of **4** was 10-fold faster (2.2 x 10^5 $M^{-1}s^{-1}$) and off-rate slower than **3** (0.00057 s^{-1}), leading to a RT of 29 minutes. The values for **3** and **4** indicate reversible binding behavior which is in line with the displacement experiments. The shape of the competition association curve of **2** (Fig. 2B) is typical for an irreversible interaction, similar to that seen recently with the irreversibly binding FSCPX at the adenosine A_1 receptor.[31] As the values determined for k_{on} and k_{off} of **2** are far from the kinetic parameters of the radioligand and beyond the duration of the experiments, they should be considered approximate values. Still, this does not change the conclusion of an infinite RT. Furthermore, **2** can be used as a tool compound for studying binding kinetics of allosteric modulators at the $mGlu_2$ receptor, a strategy that was followed before for the adenosine A_1 receptor.[32]

To distinguish between irreversible and pseudo-irreversible interactions of **2-4** we performed radioligand binding assays followed by extensive washing steps. A washout assay was developed in which 1 hour pre-incubation with a 10 x IC_{50} concentration of compound was followed by at least three extensive wash and centrifugation cycles. After the subsequent incubation with [^{3}H]JNJ-46281222, radioligand displacement was assessed and compared to the control condition without any competitor (100% radioligand binding). For **1** (unlabeled

JNJ-46281222), no radioligand displacement was found, indicating that **1** was completely washed away (Fig. 2C). For compound **3** and **4**, [^{3}H]JNJ-46281222 was displaced partially, indicating that a portion of the receptor population was still bound but no persistent covalent interactions occurred. This partial recovery of **3** and **4** was likely caused by their slower binding kinetics compared to **1**. Pre-incubation with compound **2** completely abolished [^{3}H] JNJ-46281222 binding after the washing cycles, indicating its irreversible binding to the $mGlu_2$ receptor (Fig. 2C). This was further confirmed by pre-incubation with increasing concentrations of **2**, followed by four extensive washing cycles. For this effect a concentration-response curve was established, with an apparent pK_i value for **2** of 6.63 ± 0.14 which is another qualitative assessment of the irreversible interaction.

To evaluate the effect of irreversible binding of **2** on the functional PAM response, the following [^{35}S]GTPγS set up was used. Increasing concentrations of **2** and a glutamate concentration equivalent to its EC_{20} value were pre-incubated with membranes for three hours, followed by a 1 hour incubation with [^{35}S]GTPγS, resulting in a potency of 6.75 ± 0.13, which was 7-fold higher than when co-incubation only was performed (pEC_{50} 5.90 ± 0.08) (Fig 3A). The pEC_{50} value determined after 3 hour pre-incubation followed by 1 hour co-incubation with [^{35}S]GTPγS (6.75 ± 0.13) was similar to the potency assessed in the standard [^{35}S]GTPγS protocol (6.80 ± 0.06), which also included a pre-incubation step.

The ability of bound **2** to behave as a PAM was studied by repeating the washout assay but with a [^{35}S]GTPγS binding assay subsequent to the washing cycles (Fig. 3B). Compound **2** was still able to induce [^{35}S]GTPγS binding in the presence of an EC_{20} concentration of glutamate after the washing steps. The level was comparable to the control situation in which the compound was added after the washing steps. As a further control, the assay was also performed using **1**, which did not induce [^{35}S]GTPγS binding as it was washed away (Fig. 2C), in contrast to the situation in which **1** was added after washing (Fig. 3B).

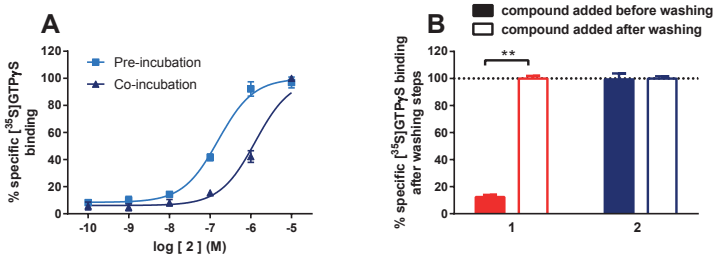

Figure 3. A.) Compound-induced [^{35}S]GTPγS binding after 60 min of incubation with [^{35}S]GTPγS with or without a 3 hour pre-incubation in the presence of a glutamate concentration equivalent to its EC_{20} value. B.) [^{35}S]GTPγS binding after stimulation with a 10x IC_{50} concentration of $mGlu_2$ PAM which was added either before or after 4 extensive washing cycles. All experiments were performed in the presence of a glutamate concentration equivalent to its EC_{20} value. Data represent the mean ± SEM of at least three individual experiments performed in duplicate. ** p<0.0001, unpaired student's t-test.

COMPUTATIONAL MODELLING

It is well understood that allosteric modulators of mGlu receptors bind in the 7TM domain in a similar conserved site as class A GPCRs.[7] Crystallography has shown variation in the exact location of allosteric ligands in this site.[33] Our previous experimental and computational studies have helped to pinpoint the binding mode of $mGlu_2$ receptor PAMs of several chemical series.[15,16] This work greatly helped the design of molecules **2** to **4**. With a strong certainty that the triazolopyridine core binds deepest in the receptor as described in **chapter 2** and by Pérez-Benito *et al.* (2017)[16] we designed and docked multiple different candidate fluorosulfonyl-phenyl molecules. Idea molecules were docked into a homology model of the $mGlu_2$ receptor allosteric binding site using a model and approach as described previously.[16,23] Due to flexibility and sequence differences there is increased uncertainty of the amino acid position and conformation in the extracellular side of the receptor model. From the docking, **2** to **4** allowed the fluorosulfonyl to explore different vectors and depths of the extracellular side of the binding site. Our approach relying upon a model of the ligand receptor binding mode, and not a crystal structure, was more high risk. Therefore, we chose the fluorosulfonyl-phenyl as the warhead because it can react with various nucleophilic amino acids as to increase the chance to find a covalent ligand.

The docking results for molecule **2** showed the triazolopyridine core overlapped with that of **1** (Fig. 4), which was included in earlier reports. As mentioned, this positioning and orientation of the scaffold is consistent with previous SAR and mutagenesis work.[34] The flexible distal tail of **2** containing the fluorosulfonyl moiety was pointing towards the top of transmembrane helices 3 or 7 and extracellular loop (ECL) 2. As suggested by the $mGlu_1$ structure, ECL2 forms a lid on top of the 7TM pocket in all class C GPCRs, which is likely happening to $mGlu_2$ as well.[10,35] Whilst the scaffold consistently adopted the shown binding orientation, two different binding modes were possible for the distal part of the molecule (Fig. 4). In the first binding mode, the distal phenyl relaxes into the 7TM of the receptor. This is analogous to the binding mode and behavior of **1** reported in the computational studies described in **chapter 2**, as shown comparing pale blue and dark orange molecules in figure 4. The fluorosulfonyl moiety is presented close to $T791^{7.29x30}$ located in our model at the top of TM-7. If the ligand maintains a more linear orientation, it will present a second possible binding mode as shown in pale orange in figure 4, where the fluorosulfonyl group points towards two alternative arginines: $R635^{3.32x32}$ and R720 (ECL2).

RECEPTOR MUTAGENESIS

Based on the two potential binding modes of **2**, multiple nucleophilic amino acid residues were within a radius of 4 Å to the fluorosulfonyl warhead and hence were potential candidates to form the covalent bond with the fluorosulfonyl. Although arginines are not widely reported to behave as nucleophiles the proximity of several in the extracellular region may permit some to be less protonated and we therefore did not want to overlook this possi-

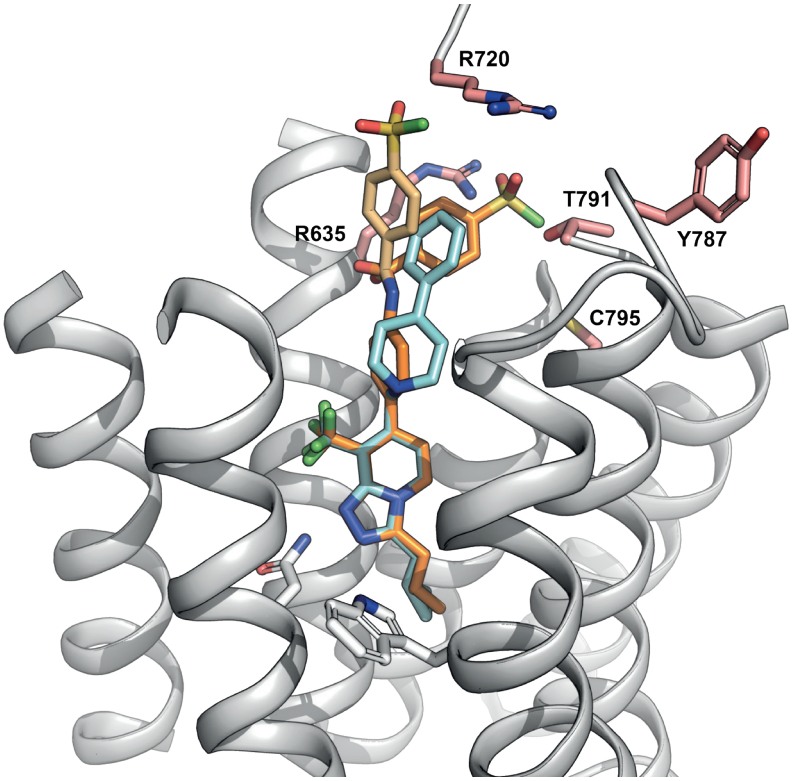

Figure 4. Proposed binding mode of $mGlu_2$ PAMs **1** (pale blue) and **2** (dark and pale orange). The two possible binding modes for **2** are distinguished using dark and pale orange coloring. The five amino acids chosen as possible candidates for the covalent interaction are highlighted in salmon color and labelled.

bility. The amino acids included R635$^{3.32x32}$ and R720 (ECL2), and T791$^{7.29x30}$. Meanwhile, Y787 (ECL3) and C795$^{7.33x34}$ were further away but given the flexibility of the extracellular region of the receptor they were still considered as possible candidates for interaction with the ligand warhead.

For all these five residues alanine substitutions were made. These $mGlu_2$ receptor mutants were transiently transfected into CHO-K1 cells and membrane preparations were made.

Control experiments confirmed the integrity and function of the mutant receptors, as shown in the supporting information (Fig. S1; Table S2). [^{3}H]LY341495 binding experiments were performed to assess the expression of transiently transfected WT and mutant $mGlu_2$ receptors, revealing a similar affinity of glutamate for the WT and all mutants, which confirmed the integrity of the orthosteric binding pocket. All mutants were still able to induce [^{35}S]GTPγS binding upon stimulation by glutamate with similar potencies, which confirmed the function of the receptor was maintained. Furthermore, all mutants were still able to bind [^{3}H]

JNJ-46281222, which was displaced by unlabeled **1** with similar affinities, which confirmed the integrity of the allosteric binding site (Fig. S1; Table S2).

To evaluate which of the amino acid residues was responsible for covalent binding of **2**, the washout assay was repeated (Fig 5A). Compound **1** was used as a control and showed around maximal [^{3}H]JNJ-46281222 binding after washing in all cases, confirming that **1** was washed away during the washing cycles. The transiently transfected WT $mGlu_2$ showed a similar effect of **2** after washing compared to the stable CHO-K1_$hmGlu_2$ cell line, i.e. complete inhibition of [^{3}H]JNJ-46281222 binding. Mutants R635$^{3.32x32}$A, R720A, Y787A and C795$^{7.33x34}$A showed a similar negligible level of [^{3}H]JNJ-46281222 binding, indicating that **2** was still binding covalently. However, T791$^{7.29x30}$A showed [^{3}H]JNJ-46281222 binding to all available binding sites, and thus a loss of covalent binding.

A full curve [^{3}H]JNJ-46281222 displacement assay using the T791$^{7.29x30}$A mutant revealed a pK_i for **2** of 6.45 ± 0.03 (Fig. 5C), which was similar to the transiently transfected WT $mGlu_2$ receptor (Fig. 5B; 6.76 ± 0.04), but lower than the pK_i found at the CHO-K1_$hmGlu_2$ membranes (Table 3). This discrepancy is likely caused by the difference in technique used, a filtration binding assay in contrast to an SPA assay.

The loss of irreversible interaction for the T791$^{7.29x30}$A mutant was further confirmed in the displacement assay, as the [^{3}H]JNJ-46281222 displacement curves of **2** with and without pre-incubation step lost the large shift shown on the WT receptor (Fig. 5C) and were almost overlapping for this mutant (Fig. 5B), indicating a loss of insurmountable binding behavior. Together, these experiments indicated that T791$^{7.29x30}$ was the residue responsible for making the covalent bond between the receptor and **2**. A similar approach was used recently for the adenosine A_{2A} and neurotensin NTS1 receptors where a lysine and cysteine residue were found to be responsible for the covalent interaction, respectively.[27,36] The position of the covalent bond was used to predict the binding mode of **2**, which further increased the understanding of the binding of PAMs to the binding pocket in addition to our recent mutagenesis and computational work described in **chapter 2** and elsewhere.[15,16,18]

Compound **2** can be a useful structural biology tool as it would be expected to stabilize the 7TM domain in its active state, thereby potentially facilitating crystallization of the active state receptor. This could be highly valuable for structure elucidation of an active state of a Class C GPCR which up to now remains unreported. Furthermore, there is no crystal structure of the 7TM domain of the $mGlu_2$ receptor. Thus far the crystal structures of class C 7TM domains were the NAM bound structures of $mGlu_1$ and $mGlu_5$.[10–12] A PAM bound structure would greatly enhance our understanding of the activation mechanism of class C GPCRs. Recently Gregory *et al.* (2016) published the first clickable covalent photo-affinity ligands for the $mGlu_5$ receptor.[37] These ligands are NAMs for the receptor and bind the receptor covalently upon

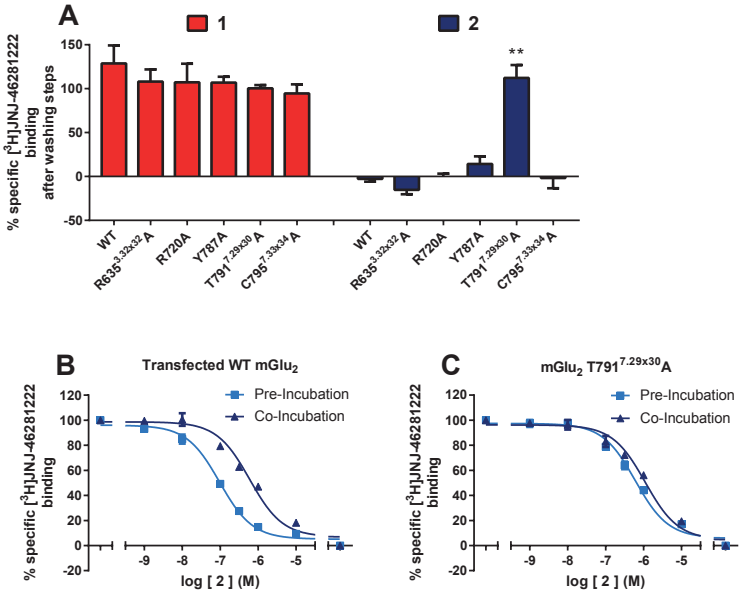

Figure 5. A.) [^{3}H]JNJ-46281222 binding to transiently transfected mGlu$_2$ mutants after pre-incubation with **1** or **2** at a 10x IC$_{50}$ concentration followed by 4 extensive washing cycles. B, C.) Displacement of specific [^{3}H]JNJ-46281222 binding from transiently transfected WT (B) and T791$^{7.29x30}$A (C) mGlu$_2$ receptor by **2** with and without a pre-incubation of 3 hours. Experiments were performed in the presence of a glutamate concentration equivalent to its EC$_{20}$ value. Data represent the mean ± SEM of at least three individual experiments performed in duplicate. ** p<0.0001, one-way ANOVA with Dunnett's post-test compared to WT.

photo-activation. The ligands contain an alkyne click handle that can be used for conjugation of clickable dyes. These probes can then be used for various purposes such as imaging in native tissues.[37] Such a strategy is also of interest for the mGlu$_2$ receptor and **2** may be used as a starting point for further chemical optimization.

Covalent ligands have proved to be successful medicines for various indications, but due to safety concerns they are mostly neglected in drug discovery.[38] This is especially the case for neuroscience indications that often require chronic treatment thus exacerbating such fears. Nevertheless, the introduction of covalent warheads into ligands that were optimized for non-covalent affinity may overcome some of the expected difficulties of off-target-activities. Such highly targeted, selective covalent inhibitors represent the current state of the art.[39] Furthermore, covalent allosteric modulators are even more likely to be used as therapeutics compared to orthosteric ligands since they lack intrinsic efficacy, thereby avoiding problems due to on-target toxicity.[40]

CONCLUSION

In conclusion, this study reports the design, synthesis and pharmacological characterization of the first covalent PAM for a class C GPCR. In addition, a combined computational and mutagenesis approach enabled the identification of T791$^{7.29x30}$ as the position of the covalent interaction. Due to its favorable allosteric properties, this compound may be considered a tool compound to further evaluate the use of covalent ligands as potential GPCR therapeutics. Furthermore, it enhances the understanding of the binding mode of PAMs, may be considered a starting point of further development of a functionalized PAM probe, and could be a valuable tool compound for structure elucidation of the $mGlu_2$ receptor.

EXPERIMENTAL SECTION

Chemistry

Unless otherwise noted, all reagents and solvents were obtained from commercial suppliers and used without further purification. Thin layer chromatography (TLC) was carried out on silica gel 60 F254 plates (Merck). Flash column chromatography was performed on silica gel, particle size 60 Å, mesh = 230–400 (Merck), under standard techniques. Microwave assisted reactions were performed in a single-mode reactor, Biotage Initiator Sixty microwave reactor (Biotage), or in a multimode reactor, MicroSYNTH Labstation (Milestone, Inc.). Nuclear magnetic resonance (NMR) spectra were recorded with either a Bruker DPX-400 or a Bruker AV-500 spectrometer (Bruker AG) with standard pulse sequences NMR data operating at 400 and 500 MHz, respectively, using $CDCl_3$ and DMSO-d_6 as solvents. Chemical shifts (δ) are reported in parts per million (ppm) downfield from tetramethylsilane (δ = 0). Coupling constants are reported in hertz. Splitting patterns are defined by s (singlet), d (doublet), dd (double doublet), t (triplet), q (quartet), quin (quintet), sex (sextet), sep (septet), or m (multiplet). Liquid chromatography combined with mass spectrometry (LC–MS) was performed either on a HP 1100 HPLC system (Agilent Technologies) or Advanced Chromatography Technologies system composed of a quaternary or binary pump with degasser, an autosampler, a column oven, a diode array detector (DAD), and a column as specified in the respective methods. Flow from the column was split to a MS spectrometer. The MS detector was configured with either an electrospray ionization source or an ES-CI dual ionization source (electrospray combined with atmospheric pressure chemical ionization). Nitrogen was used as the nebulizer gas. Data acquisition was performed with MassLynx- Openlynx software or with Chemstation-Agilent Data Browser software.

Compounds are described by their experimental retention times (Rt) and ions. The reported molecular ion corresponds to the [M+H]+ (protonated molecule) and/or [M-H]- (deprotonated molecule). Purities of all new compounds were determined by analytical RP-HPLC using the area percentage method on the UV trace recorded at a wavelength of 254 nm, and compounds were found to have ≥95% purity unless otherwise specified. For (LC)MS-characterization of the compounds of the present manuscript, the following method was used.

General procedure

The High Performance Liquid Chromatography (HPLC) measurement was performed using an LC pump, a diode-array (DAD) or a UV detector and a column as specified in the respective methods. If necessary, additional detectors were included (see table of methods below). Flow from the column was brought to the Mass Spectrometer (MS) which was configured with an atmospheric pressure ion source. It is within the knowledge of the skilled person to set the tune parameters (e.g. scanning range, dwell time…) in order to obtain ions allowing the identification of the compound's nominal monoisotopic molecular weight (MW) and/or exact mass monoisotopic molecular weight. Data acquisition was performed with appropriate software. Compounds are described by their experimental retention times (R_t) and ions. If not specified differently in the table of data, the reported molecular ion corresponds to the $[M+H]^+$ (protonated molecule) and/or $[M-H]^-$ (deprotonated molecule). In case the compound was not directly ionizable the type of adduct is specified (i.e. $[M+NH_4]^+$, $[M+HCOO]^-$, etc…). For molecules with multiple isotopic patterns (Br, Cl..), the reported value is the one obtained for the lowest isotope mass. All results were obtained with experimental uncertainties that are commonly associated with the method used. Hereinafter, "DAD" means Diode Array Detector, "SQD" Single Quadrupole Detector, "CSH", Charged Surface Hybrid.

Method 1

In addition to the general procedure: Reversed phase HPLC was carried out on an Eclipse Plus-C18 column (3.5 µm, 2.1 x 30 mm) from Agilent, with a flow rate of 1.0 ml/min, at 60ºC without split to the MS detector. The gradient conditions used are: 95 % A (0.5 g/l ammonium acetate solution + 5 % acetonitrile), 5 % B (mixture of acetonitrile / methanol, 1/1), kept 0.2 minutes, to 100 % B at 1.0 minute, kept till 1.15 minutes and equilibrated to initial conditions at 1.3 minutes, kept until 3.0 minutes. Injection volume 2 µl. Low-resolution mass spectra (single quadrupole, SQD detector) were acquired by scanning from 100 to 1000 in 0.1 seconds using an inter-channel delay of 0.08 second. The capillary needle voltage was 3 kV. The cone voltage was 20 V for positive ionization mode and 30 V for negative ionization mode. This method was used for compounds **7a-c**.

Method 2

In addition to the general procedure: Reversed phase UPLC was carried out on an CSH -C18 column (1.7 µm, 2.1 x 50 mm) from Waters, with a flow rate of 1.0 ml/min, at 50ºC without split to the MS detector. The gradient conditions used are: 95 % A (0.5 g/l ammonium acetate solution + 5 % acetonitrile), 5 % B (acetonitrile), to 95 % B at 4.6 minutes, kept until

5.0 minutes. Injection volume 2 µl. Low-resolution mass spectra (single quadrupole, SQD detector) were acquired by scanning from 100 to 1000 in 0.1 seconds using an inter-channel delay of 0.08 second. The capillary needle voltage was 3 kV. The cone voltage was 25 V for positive ionization mode and 30 V for negative ionization mode. This method was used for compounds **2-4.**

4-[[4-[3-(Cyclopropylmethyl)-8-(trifluoromethyl)-[1,2,4]triazolo[4,3-a]pyridin-7-yl]phenyl]carbamoyl] benzenesulfonyl fluoride (2). DIPEA (0.079 mL, 0.4514 mmol) was added to a stirred solution of **7a** (0.1 g, 0.301 mmol), **8a** (0.074 mg, 0.3611 mmol) and HATU (0.195 mg, 0.512 mmol) in DMF (2 mL). The mixture was stirred at room temperature for 3 hours. The mixture was diluted with CH_2Cl_2 and washed with sat. NH_4Cl and $NaHCO_3$ aqueous saturated solution. The organic layer was separated, dried (Na_2SO_4), filtered and the solvents evaporated in vacuo. The crude product was purified by flash column chromatography (silica; CH_2Cl_2 in MeOH 100/0 to 94/6). The desired fractions were collected and the solvents evaporated in vacuo to yield **2** (0.116 g, 75%). ^{1}H NMR (500 MHz, DMSO-d_6) δ 10.84 (s, 1H), 8.75 (d, *J*=7.22 Hz, 1H), 8.22-8.41 (m, 4H), 7.93 (d, *J*=8.38 Hz, 2H), 7.47 (d, *J*=8.67 Hz, 2H), 6.97 (d, *J*=6.94 Hz, 1H), 3.15 (d, *J*=6.94 Hz, 2H), 1.19-1.31 (m, 1H), 0.46-0.66 (m, 2H), 0.23-0.41 (m, 2H). LC-MS: m/z 519 $[M + H]^+$, *t*R = 2.24 min.

4-[[3-[3-(Cyclopropylmethyl)-8-(trifluoromethyl)-[1,2,4]triazolo[4,3-a]pyridin-7-yl]phenyl]carbamoyl] benzenesulfonyl fluoride (3). Starting from **7b** (0.260 g, 0.7824 mmol) and **8b** (0.192 mg, 0.9388 mmol) and following the procedure described for **2**, compound **3** was obtained (0.274 g, 68%). ^{1}H NMR (500 MHz, DMSO-d_6) δ 10.83 (s, 1H), 8.76 (d, *J*=7.22 Hz, 1H), 8.22-8.42 (m, 4H), 7.81-7.99 (m, 2H), 7.54 (t, *J*=7.80 Hz, 1H), 7.21 (d, *J*=7.80 Hz, 1H), 6.96 (d, *J*=7.22 Hz, 1H), 3.15 (d, *J*=6.65 Hz, 2H), 1.12-1.37 (m, 1H), 0.46-0.66 (m, 2H), 0.23-0.42 (m, 2H). LC-MS: m/z 519 $[M + H]^+$, *t*R = 2.24 min.

4-[[4-[3-(Cyclopropylmethyl)-8-(trifluoromethyl)-[1,2,4]triazolo[4,3-a]pyridin-7-yl]phenyl]methylcarbamoyl] benzenesulfonyl fluoride (4). 7c (0.050g, 0.144 mmol) in 1,4-dioxane (0.5 mL) was added to **8b** (0.038 g, 0.173 mmol). The resulting suspension was heated at 90ºC for 30 min. After cooling, the suspension was filtered, washed with Et_2O and dried under vacuum. The crude product was purified by flash column chromatography (silica; CH_2Cl_2 in MeOH 100/0 to 94/6) to give **4** as a white solid. (0.025 g, 33%). ^{1}H NMR (400 MHz, DMSO-d_6) δ 9.55 (t, *J*=5.90 Hz, 1H), 8.73 (d, *J*=6.94 Hz, 1H), 8.13-8.39 (m, 4H), 7.31-7.55 (m, 1H), 6.92 (d, *J*=7.40 Hz, 1H), 4.62 (d, *J*=6.01 Hz, 2H), 3.13 (d, *J*=6.70 Hz, 2H), 1.14-1.31 (m, 2H), 0.45-0.62 (m, 2H), 0.20-0.40 (m, 2H). LC-MS: m/z 533 $[M + H]^+$, *t*R = 2.13 min.

4-[3-(Cyclopropylmethyl)-8-(trifluoromethyl)-[1,2,4]triazolo[4,3-a]pyridin-7-yl]aniline (7a). $Pd(PPh_3)_4$ (0.075 g, 0.065 mmol) was added to a stirred suspension of **5** (0.300 g, 1.0883 mmol) and **6a** (0.164 g, 1.197 mmol) in a saturated aqueous solution of $NaHCO_3$ (2 mL) and 1,4-dioxane (5 mL). The mixture was heated at 150 °C for 15 min under microwave irradiation, then cooled to room temperature and filtered through a Celite pad. The filtrate was diluted with water (20 mL) and extracted with EtOAc (2 × 15 mL). The organic layer was washed with brine (15 mL), dried over anhydrous Na_2SO_4, and concentrated in vacuo. The crude was purified by flash column chromatography (silica gel, MeOH–NH_3 in CH_2Cl_2, 0/100 to 5/95) to give the desired product **7a** as a pale yellow solid (0.227 g, 61%). LC-MS: m/z 333 $[M + H]^+$, *t*R = 1.62 min.

3-[3-(Cyclopropylmethyl)-8-(trifluoromethyl)-[1,2,4]triazolo[4,3-a]pyridin-7-yl]aniline (7b). Starting from **5** (0.300 g, 1.0883 mmol) and **6b** (0.208 g, 1.197 mmol) and following the procedure described for **7a**, compound **7b** was obtained as a pale yellow solid (0.265 g, 68%). LC-MS: m/z 333 $[M + H]^+$, *t*R = 1.64 min.

[4-[3-(Cyclopropylmethyl)-8-(trifluoromethyl)-[1,2,4]triazolo[4,3-a]pyridin-7-yl]phenyl]methanamine (7c). Starting from **5** (0.300 g, 1.0883 mmol) and **6c** (0.279 g, 1.197 mmol) and following the procedure described for **7a**, compound **7c** was obtained as a pale yellow solid (0.245 g, 65%). LC-MS: m/z 347 [M + H]+, tR = 1.5 min.

Biology

Cell Culture

CHO-K1 cells (CCL-61; ATCC, Rockville, MD, USA) were grown in Dulbecco's modified Eagle's medium/Nutrient F-12 Ham (DMEM/F12) supplemented with 10% (v/v) fetal calf serum, 100 IU·mL^{-1} penicillin, 100 µg·mL^{-1} streptomycin and 100 mM pyruvate. CHO-K1 cells

stably expressing the wildtype (WT) hmGlu$_2$ receptor (CHO-K1_hmGlu$_2$; Janssen Research and Development) were grown in Dulbecco's modified Eagle's medium (DMEM) supplemented with 10% (v/v) fetal calf serum, 200 IU·mL^{-1} penicillin, 200 μg·mL^{-1} streptomycin, 30.5 μg·mL^{-1} L-proline and 400 μg·mL^{-1} G418. All cells were grown at 37°C and 5% CO_2 and were subcultured at a ratio of 1:10 twice every week.

Plasmids and Transient Transfection

cDNA encoding human mutated and non-mutated mGlu$_2$ receptors was synthesized by GeneArt® (Life Technologies, Carlsbad, CA, USA), subcloned to the pcDNA3.1(+) expression vector (Life Technologies) and amplified by *E. Coli* transformation. 24 hours before transfection, cells were seeded in 15 cm Ø culture plates at high density (20,000 cells/cm^2). Transient transfections in CHO-K1 cells were performed using the cationic lipid transfection reagent LTX lipofectamine reagent (Life Technologies).

Cell Membrane Preparation

CHO-K1_hmGlu$_2$ cells in DMEM without G418 were plated into 15 cm Ø plates. Upon growth to 70% confluency sodium butyrate (final concentration 5 mM) was added to the plates [41]. After 24 hours, cells were detached by scraping into 5 ml of PBS and subsequently centrifuged at 1500 rpm for 5 min. Pellets were resuspended in ice-cold Tris buffer (50 mM Tris-HCl pH 7.4) and homogenized using an Ultra Turrax homogenizer at 24,000 rpm (IKA-Werke GmbH & Co.KG, Staufen, Germany). Membranes and the cytosolic fraction were separated by centrifugation at 31,000 rpm at 4°C for 20 min in an Optima LE-80 K ultracentrifuge (Beckman Coulter, Fullerton, CA). After resuspension of pellets in 10 ml Tris buffer, the centrifugation and homogenization steps were repeated. The remaining pellets were suspended into assay buffer (50 mM Tris-HCl pH 7.4, 2 mM $CaCl_2$, 10 mM $MgCl_2$) which was followed by homogenization. Aliquots were stored at -80°C.

[^{3}H]JNJ-46281222 binding assays using CHO-K1_hmGlu$_2$ membranes

Membrane homogenates (15 μg) and pre-wetted wheat-germ agglutinin coated SPA beads (0.2 mg; RPNQ0001, PerkinElmer, Groningen, The Netherlands) were pre-coupled in assay buffer while gently shaking at room temperature for 30 minutes. Then, this membrane bead mixture was added to an Isoplate-96 (PerkinElmer) together with 6 nM [^{3}H]JNJ-46281222 and increasing concentrations of competing ligand. Nonspecific binding was determined using 10 μM JNJ-40068782 (**9**)[42]. In case of pre-incubation experiments, [^{3}H]JNJ-46281222 was added after a 3 hour pre-incubation of the samples containing membrane and competitor. Plates were counted in a Microbeta 2450^2 Trilux scintillation microplate counter (PerkinElmer) after a 1 hour incubation at 25°C.

For competition association experiments, the plate was rapidly placed in the microplate counter after addition of the membrane homogenates. Plates were recorded for 120 minutes

measuring every 30 seconds at ambient temperature. The assay buffer in these experiments contained 1 mM glutamate, as this was shown to induce monophasic association and dissociation. This enabled straightforward determination of kinetic parameters and resembles a condition at which PAMs likely exert their effect under physiological conditions.[18]

[^{3}H]JNJ-46281222 binding assays using transiently transfected CHO-K1 hmGlu$_2$ membranes

Membrane homogenates (30 or 60 μg) were diluted in ice-cold assay buffer (50 mM Tris-HCl pH 7.4, 2 mM $CaCl_2$, 10 mM $MgCl_2$) to a total reaction volume of 100 μl containing increasing concentrations of competing ligand and 6 nM [^{3}H]JNJ-46281222. Nonspecific binding was determined using 10 μM **9**. After 1 hour at 15°C, incubation was terminated by rapid filtration over GF/C filters through a Brandel harvester 24 (Brandel, Gaithersburg, MD, USA) Filters were subsequently washed at least three times using ice-cold wash buffer (50 mM TRIS-HCl pH 7.4). Filter-bound radioactivity was determined using liquid scintillation spectrometry on a TRI-Carb 2810 TR counter (PerkinElmer).

Irreversible binding of [^{3}H]JNJ-46281222 to CHO-K1_hmGlu$_2$ and transiently transfected hmGlu$_2$ membranes.

Membrane homogenates (30, 60 or 120 μg) were chosen such that specific binding was close to 10% to allow for good resolution and avoid ligand depletion. Samples were incubated with mGlu$_2$ PAMs **1**-**4** at a 10x IC_{50} concentration in a total volume of 400 μl (CHO-K1_hmGlu$_2$ membranes) assay buffer containing 1 mM glutamate in Eppendorf tubes. 0.25% DMSO was taken as a control for total binding and non-specific binding.

After incubation for 1 hour at 25°C while gently shaking, the samples were centrifuged at 16,100x*g* at 4°C for 5 minutes. Unbound ligands were removed by aspiration of supernatant. 1 ml of assay buffer was added, pellets were resuspended and samples were incubated for 20 min. at 25°C. This centrifugation and washing cycle was repeated 4 times. After that, supernatant was removed and the membranes were resuspended in a total volume of 400 μl (CHO-K1_hmGlu$_2$) or 100 μl (transiently transfected hmGlu$_2$ mutants) containing 6 nM [^{3}H] JNJ-46281222 and 1 mM glutamate in tubes. Non-specific binding was determined using 10 μM **9**. After 1 hour incubation at 25°C, incubations were terminated and samples obtained and analyzed as described under '*[^{3}H]JNJ-46281222 Binding*'.

[^{35}S]GTPγS Binding Assays

Membrane homogenates (5 or 10 μg) were diluted in ice-cold assay buffer (50 mM Tris-HCl pH 7.4, 100 mM NaCl, 3 mM $MgCl_2$) supplemented with 10 μM GDP (Sigma-Aldrich, St. Louis, MO, USA) and 5 μg saponin to a total reaction volume of 80 μl containing increasing concentrations of ligand of interest and a glutamate concentration equivalent to its EC_{20} value (4 μM) in case of a PAM dose-response curve. Basal receptor stimulation was determined using assay buffer, maximum receptor stimulation was determined using 1 mM glutamate.

Samples were pre-incubated for 30 minutes at 25 °C. Subsequently, 20 µl [^{35}S]GTPγS (final concentration 0.3 nM; PerkinElmer) was added. The reaction was stopped after a 90 minute incubation at 25 °C by rapid filtration through a 96-well GF/B filterplate (PerkinElmer) on a PerkinElmer filtermate harvester. Plates were washed with ice-cold wash buffer (50 mM Tris-HCl pH 7.4, 5 mM $MgCl_2$). Filter-bound radioactivity was determined by scintillation spectrometry using the Microbeta^2 counter.

Irreversible binding to CHO-K1_hmGlu$_2$ membranes in a functional [^{35}S]GTPγS binding assay.

Experiments were performed as described under '*Irreversible binding of [^{3}H]JNJ-46281222 to CHO-K1_hmGlu$_2$ and transiently transfected mutant hmGlu$_2$ membranes'*, with assay buffer as described under '*[^{35}S]GTPγS Binding'*. PAMs were diluted in assay buffer containing a glutamate concentration equivalent to its EC_{20} value (4 µM). After the washing steps, membrane suspensions were transferred to tubes in a volume of 360 µl assay buffer containing saponin (10 µg) and GDP (10 µM). PAM samples contained an EC_{20} glutamate concentration, total binding was determined using 1 mM glutamate and basal [^{35}S]GTPγS binding was determined using assay buffer only. Samples were pre-incubated for 30 minutes at 25 °C. Subsequently, 40 µl [^{35}S]GTPγS (final concentration 0.3 nM) was added. The reaction was stopped after a 30 minute incubation at 25 °C by rapid filtration over GF/B filters through a Brandel harvester 24 (Brandel, Gaithersburg, MD, USA). Filters were subsequently washed at least three times using ice-cold wash buffer (50 mM Tris-HCl pH 7.4, 5 mM $MgCl_2$). Samples were analyzed as described under '*[^{3}H]JNJ-46281222 Binding*'.

[^{3}H]LY341495 Binding Assays

Membrane homogenates (5 µg) were diluted in assay buffer (50 mM Tris-HCl pH 7.4, 2 mM $CaCl_2$, 10 mM $MgCl_2$) to a total reaction volume of 100 µl containing increasing concentrations of glutamate (100 nM to 1 mM) and 3 nM [^{3}H]LY341495 (ARC, St. Louis, MO, USA). Non-specific binding was determined using 1 mM glutamate. After incubation for 1 hour at 25°C, samples were rapidly filtered through a 96-well GF/B filterplate (PerkinElmer) on a PerkinElmer filtermate harvester and washed three times with ice-cold wash buffer (50 mM Tris-HCl pH 7.4). Samples were analyzed as described under '*[^{3}H]JNJ-46281222 Binding*'.

For all radioligand binding experiments DMSO concentrations were ≤0.25% and radioligand concentrations were chosen such that <10% of the amount added was receptor-bound to avoid ligand depletion.

Data analysis

Data analyses were performed using Prism 7.00 (GraphPad software, San Diego, CA, USA). pIC_{50} values were obtained using non-linear regression curve fitting into a sigmoidal concentration-response curve using the equation: Y=Bottom + (Top-Bottom)/(1+10^(X-LogIC$_{50}$)). pK_i values were obtained from pIC_{50} values using the Cheng-Prusoff equation [43]. pEC_{50} values were

determined using non-linear regression curve fitting into a sigmoidal concentration-response curve with variable slope using the equation: Y=Bottom + (Top-Bottom)/(1+10$^{((LogEC50-X)*Hillslope)}$). Association and dissociation rate constants for unlabeled mGlu$_2$ PAMs were determined by nonlinear regression analysis of competition association data as described by Motulsky and Mahan.[30] In these equations k_1 and k_2 represent the k_{on} and k_{off} of [^{3}H]JNJ-46281222, which are described in table 1.

$$K_A = k_1[L]\cdot 10^{-9} + k_2$$
$$K_B = k_3[I]\cdot 10^{-9} + k_4$$
$$S = \sqrt{(K_A - K_B)^2 + 4\cdot k_1\cdot k_3\cdot L\cdot I\cdot 10^{-18}}$$
$$K_F = 0.5(K_A + K_B + S)$$
$$K_S = 0.5(K_A + K_B - S)$$
$$Q = \frac{B_{max}\cdot k_1\cdot L\cdot 10^{-9}}{K_F - K_S}$$
$$Y = Q\cdot\left(\frac{k_4\cdot(K_F - K_S)}{K_F\cdot K_S} + \frac{k_4 - K_F}{K_F}e^{(-K_F\cdot X)} - \frac{k_4 - K_S}{K_S}e^{(-K_S\cdot X)}\right)$$

Data shown represent the mean ± SEM of at least three individual experiments performed in duplicate. Statistical analysis was performed if indicated, using a one-way ANOVA with Dunnett's post-test or an unpaired student's t-test. Observed differences were considered statistically significant if p-values were below 0.05.

Computational efforts

The mGlu$_2$ receptor homology model: Method is as described in **chapter 2**. An active state model of the 7TM domain of human mGlu$_2$ receptor (Uniprot code Q14416) bound to G protein was built using a combination of structural templates. The crystal structure of the human mGlu$_5$ (PDB 4OO9, [11]) was used to model all 7TM helices except TM6. ECL2 is not refined in the mGlu$_5$ X-ray structure therefore this important loop was modelled based on the mGlu$_1$ receptor crystal structure (PDB 4OR2, [10]). Finally, the β_2AR (PDB ID 3SN6, [44]) active structure was used to model both TM6 in its distinct open conformation as well as the corresponding G protein. The sequence identity between mGlu$_2$ and mGlu$_5$ 7TM's is 51%. The initial model was constructed in MOE v2014.9 (Chemical computing group Inc., Montreal, QC, Canada) and then Maestro (Schrodinger LLC, New York, NY, USA) was used for structure preparation. The Protein Preparation tool was used to fix any missing sidechains/atoms, PROPKA assigned protonation states, the hydrogen bonding network was optimized, and brief minimization until no further change of RMSD to within 0.5 Å removed any structural clashes.

Docking of 2: The ligand was prepared for docking using Maestro. Conformational sampling was performed with ConfGen and multiple conformers were docked into the mGlu$_2$ active state model using Glide XP. As there is no ligand in the mGlu$_2$ model, the docking grid was centered on the ligand position in the mGlu$_1$ receptor structure, based on superposition

of $mGlu_1$ and $mGlu_2$. Sampling was increased in the Glide docking by turning on expanded sampling and passing 100 initial poses to post-docking minimization. All other docking parameters were set to the defaults.

REFERENCES

1. Weichert D, Gmeiner P. *ACS Chem Biol*. **2015**; 10: 1376–1386.

2. Nygaard R, Zou Y, Dror RO, Mildorf TJ, Arlow DH, Manglik A, Pan AC, Liu CW, Fung JJ, Bokoch MP, Thian FS, Kobilka TS, Shaw DE, Mueller L, Prosser RS, Kobilka BK. *Cell*. **2013**; 152: 532–42.

3. Glukhova A, Thal DM, Nguyen AT, Vecchio EA, Jörg M, Scammells PJ, May LT, Sexton PM, Christopoulos A. *Cell*. **2017**; 168: 867–877.e13.

4. Weichert D, Kruse AC, Manglik A, Hiller C, Zhang C, Hubner H, Kobilka BK, Gmeiner P. *Proc Natl Acad Sci*. **2014**; 111: 10744–10748.

5. Niswender CM, Conn PJ. *Annu Rev Pharmacol Toxicol*. **2010**; 50: 295–322.

6. Pin J-P, Bettler B. *Nature*. **2016**; 540: 60–68.

7. Lindsley CW, Emmitte KA, Hopkins CR, Bridges TM, Gregory KJ, Niswender CM, Conn PJ. *Chem Rev*. **2016**; 116: 6707–6741.

8. Nicoletti F, Bockaert J, Collingridge GL, Conn PJ, Ferraguti F, Schoepp DD, Wroblewski JT, Pin JP. *Neuropharmacology*. **2011**; 60: 1017–41.

9. Monn JA, Prieto L, Taboada L, Pedregal C, Hao J, Reinhard MR, Henry SS, Goldsmith PJ, Beadle CD, Walton L, Man T, Rudyk H, Clark B, Tupper D, Baker SR, Lamas C, Montero C, Marcos A, Blanco J, Bures M, Clawson DK, Atwell S, Lu F, Wang J, Russell M, Heinz BA, Wang X, Carter JH, Xiang C, Catlow JT, Swanson S, Sanger H, Broad LM, Johnson MP, Knopp KL, Simmons RM a, Johnson BG, Shaw DB, McKinzie DL. *J Med Chem*. **2015**; 58: 1776–1794.

10. Wu H, Wang C, Gregory KJ, Han GW, Cho HP, Xia Y, Niswender CM, Katritch V, Meiler J, Cherezov V, Conn PJ, Stevens RC. *Science*. **2014**; 344: 58–64.

11. Doré AS, Okrasa K, Patel JC, Serrano-Vega M, Bennett K, Cooke RM, Errey JC, Jazayeri A, Khan S, Tehan B, Weir M, Wiggin GR, Marshall FH. *Nature*. **2014**; 511: 557–62.

12. Christopher JA, Aves SJ, Bennett KA, Doré AS, Errey JC, Jazayeri A, Marshall FH, Okrasa K, Serrano-Vega MJ, Tehan BG, Wiggin GR, Congreve M. *J Med Chem*. **2015**; 58: 6653–6664.

13. Cid JM, Tresadern G, Vega JA, de Lucas AI, Matesanz E, Iturrino L, Linares ML, Garcia A, Andrés JI, Macdonald GJ, Oehlrich D, Lavreysen H, Megens A, Ahnaou A, Drinkenburg W, Mackie C, Pype S, Gallacher D, Trabanco AA. *J Med Chem*. **2012**; 55: 8770–89.

14. Cid JM, Duvey G, Tresadern G, Nhem V, Furnari R, Cluzeau P, Vega JA, de Lucas AI, Matesanz E, Alonso JM, Linares ML, Andrés JI, Poli SM, Lutjens R, Himogai H, Rocher J, Macdonald GJ, Oehlrich D, Lavreysen H, Ahnaou A, Drinkenburg W, Mackie C, Trabanco AA. *J Med Chem*. **2012**; 55: 2388–2405.

15. Farinha A, Lavreysen H, Peeters L, Russo B, Masure S, Trabanco AA, Cid J, Tresadern G. *Br J Pharmacol*. **2015**; 172: 2383–96.

16. Pérez-Benito L, Doornbos MLJ, Cordomí A, Peeters L, Lavreysen H, Pardo L, Tresadern G. *Structure*. **2017**; 25: 1–10.

17. Doornbos MLJ, Cid JM, Haubrich J, Nunes A, van de Sande JW, Vermond SC, Mulder-Krieger T, Trabanco AA, Ahnaou A, Drinkenburg WH, Lavreysen H, Heitman LH, IJzerman AP, Tresadern G. *J Med Chem*. **2017**; 60: 6704–6720.

18. Doornbos MLJ, Pérez-Benito L, Tresadern G, Mulder-Krieger T, Biesmans I, Trabanco AA, Cid JM, Lavreysen H, IJzerman AP, Heitman LH. *Br J Pharmacol*. **2016**; 173: 588–600.

19. Lavreysen H, Langlois X, Ver Donck L, Cid Nuñez JM, Pype S, Lütjens R, Megens A. *Pharmacol Res Perspect*. **2015**; 3: e00097.

20. Salih H, Anghelescu I, Kezic I, Sinha V, Hoeben E, Van Nueten L, De Smedt H, De Boer P. *J Psychopharmacol*. **2015**; 29: 414–425.

21. Kent JM, Daly E, Kezic I, Lane R, Lim P, De Smedt H, De Boer P, Van Nueten L, Drevets WC, Ceusters M. *Prog Neuro-Psychopharmacology Biol Psychiatry*. **2016**; 67: 66–73.

22. Cid JM, Tresadern G, Duvey G, Lütjens R, Finn T, Rocher J, Poli S, Vega JA, de Lucas AI, Matesanz E, Linares ML, Andrés JI, Alcazar J, Alonso JM, Macdonald GJ, Oehlrich D, Lavreysen H, Ahnaou A, Drinkenburg W, Mackie C, Pype S, Gallacher D, Trabanco AA. *J Med Chem*. **2014**; 57: 6495–512.

23. Cid JM, Tresadern G, Vega JA, De Lucas AI, Del Cerro A, Matesanz E, Linares ML, García A, Iturrino L, Pérez-Benito L, Macdonald GJ, Oehlrich D, Lavreysen H, Peeters L, Ceusters M, Ahnaou A, Drinkenburg W, Mackie C, Somers M, Trabanco AA. *J Med Chem*. **2016**; 59: 8495–8507.

24. Cid-Nuñez, J. M., De Lucas Olivares, A. I., Trabanco-Suarez, A. A., MacDonald, G. J. **2010**.

25. Narayanan A, Jones LH. *Chem Sci*. **2015**; 6: 2650–2659.

26. Nijmeijer S, Engelhardt H, Schultes S, van de Stolpe AC, Lusink V, de Graaf C, Wijtmans M, Haaksma EEJ, de Esch IJP, Stachurski K, Vischer HF, Leurs R. *Br J Pharmacol*. **2013**; 170: 89–100.

27. Yang X, Dong G, Michiels TJM, Lenselink EB, Heitman L, Louvel J, IJzerman AP. *Purinergic Signal*. **2017**; 13: 191–201.

28. Kenakin T, Jenkinson S, Watson C. *J Pharmacol Exp Ther*. **2006**; 319: 710–723.

29. Strelow JM. *SLAS Discov Adv Life Sci R&D*. **2017**; 22: 3–20.

30. Motulsky HJ, Mahan LC. *Mol Pharmacol*. **1984**; 25: 1–9.

31. Xia L, de Vries H, IJzerman AP, Heitman LH. *Purinergic Signal*. **2016**; 12: 115–126.

32. Guo D, van Dorp EJH, Mulder-Krieger T, van Veldhoven JPD, Brussee J, IJzerman AP, Heitman LH. *J Biomol Screen*. **2013**; 18: 309–20.

33. Congreve M, Oswald C, Marshall FH. *Trends Pharmacol Sci*. **2017**; xx: 1–11.

34. Tresadern G, Cid J-MM, Trabanco AA. *J Mol Graph Model*. **2014**; 53: 82–91.

35. Harpsøe K, Boesgaard MW, Munk C, Bräuner-Osborne H, Gloriam DE. *Bioinformatics*. **2017**; 33: 1116–1120.

36. Kling RC, Plomer M, Lang C, Banerjee A, Hübner H, Gmeiner P. *ACS Chem Biol*. **2016**; 11: 869–875.

37. Gregory KJ, Velagaleti R, Thal DM, Brady RM, Christopoulos A, Conn PJ, Lapinsky DJ. *ACS Chem Biol*. **2016**; 11: 1870–1879.

38. Singh J, Petter RC, Baillie TA, Whitty A. *Nat Rev Drug Discov*. **2011**; 10: 307–317.

39. Baillie TA. *Angew Chemie - Int Ed*. **2016**; 55: 13408–13421.

40. Lu S, Zhang J. *Drug Discov Today*. **2017**; 22: 447–453.

41. Cuisset L, Tichonicky L, Jaffray P, Delpech M. *J Biol Chem*. **1997**; 272: 24148–24153.

42. Lavreysen H, Langlois X, Ahnaou A, Drinkenburg W, te Riele P, Biesmans I, Van der Linden I, Peeters L, Megens A, Wintmolders C, Cid JM, Trabanco AA, Andrés JI, Dautzenberg FM, Lütjens R, Macdonald G, Atack JR. *J Pharmacol Exp Ther*. **2013**; 346: 514–27.

43. Cheng Y, Prusoff WH. *Biochem Pharmacol*. **1973**; 22: 3099–108.

44. Rasmussen SGF, DeVree BT, Zou Y, Kruse AC, Chung KY, Kobilka TS, Thian FS, Chae PS, Pardon E, Calinski D, Mathiesen JM, Shah ST a, Lyons J a, Caffrey M, Gellman SH, Steyaert J, Skiniotis G, Weis WI, Sunahara RK, Kobilka BK. *Nature*. **2011**; 477: 549–55.

SUPPORTING FIGURE AND TABLES

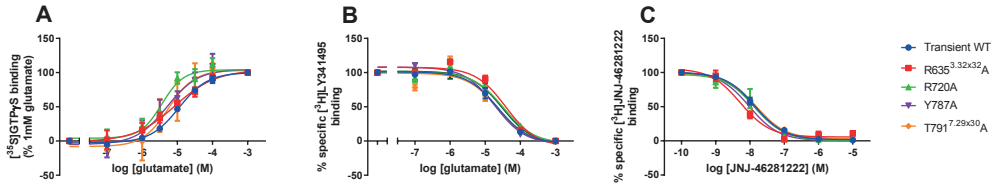

Figure S1. Effect of transiently transfected $mGlu_2$ receptor mutants on [^{35}S]GTPγS binding (A) and displacement of [^{3}H]LY341495 (B) and [^{3}H]JNJ-46281222 (C). Data represent the mean ± SEM of at least three individual experiments performed in duplicate.

Table S1. Selectivity data for representative $mGlu_2$ PAM **3** at $mGlu_{1,3,5,8}$.

Compound	$hmGlu_1$-Ago-Ca-pEC_{50}	$hmGlu_1$-Anta-Ca-pIC_{50}	$hmGlu_1$-PAM-Ca-pEC_{50}	$hmGlu_3$-Ago-Ca-pEC_{50}	$hmGlu_3$-Anta-Ca-pIC_{50}	$hmGlu_3$-PAM-Ca-pEC_{50}	$hmGlu_5$-Ago-Ca-pEC_{50}	$hmGlu_5$-Anta-Ca-pIC_{50}	$hmGlu_5$-PAM-Ca-pEC_{50}	$hmGlu_8$-Ago-Ca-pEC_{50}	$hmGlu_8$-Anta-Ca-pIC_{50}
3	<4.3	<4.3	<4.3	<4.3	<4.3	<4.3	<4.3	~4.69	<4.3	<4.3	<4.3

Ago, agonism; Anta, antagonism; PAM, positive allosteric modulation; Ca, data from calcium response in Ca^{2+}-based FDSS assay; All assays used the human receptor. Further details of methods can be found in Pérez-Benito *et al.* (2017).[16]

Table S2. Effect of transiently transfected $mGlu_2$ receptor mutants on [^{35}S]GTPγS binding and displacement of [^{3}H]LY341495 and [^{3}H]JNJ-46281222. Data represent the mean ± SEM of at least three individual experiments performed in duplicate.

	[^{35}S]GTPγS binding	[^{3}H]LY341495 displacement	[^{3}H]JNJ-46281222 displacement
Mutant	**Glutamate pEC_{50}**	**Glutamate pIC_{50}**	**JNJ-46281222 pK_i**
Transient WT	4.95 ± 0.04	5.07 ± 0.12	8.38 ± 0.13
R635$^{3.32x32}$A	4.9 ± 0.22[a]	4.84 ± 0.04	8.76 ± 0.10
R720A	5.08 ± 0.11	4.91 ± 0.03	8.51 ± 0.18
Y787A	5.43 ± 0.05	5.07 ± 0.09	8.55 ± 0.04
T791$^{7.29x30}$A	5.31 ± 0.21	5.13 ± 0.05	8.36 ± 0.07
C795$^{7.33x34}$A	5.30 ± 0.25	4.94 ± 0.06	8.42 ± 0.07

Values represent the mean ± SEM of at least three individual experiments, performed in duplicate. [a] As previously described by Farinha *et al.* (2015).[15]